

Continuous Fabrication of Free-Standing TiO_2 Nanotube Array Membranes with Controllable Morphology for Depositing Interdigitated Heterojunctions

Daqai Wang and Lifeng Liu*

Max Planck Institute of Microstructure Physics, Weinberg 2, D06120 Halle, Germany

Received September 13, 2010. Revised Manuscript Received November 4, 2010

Free-standing and through-hole TiO_2 nanotube array membranes were fabricated via a novel electrochemical in situ separation process, by taking advantage of conventional anodization of Ti, followed by the application of a large voltage pulse for a short time. The TiO_2 nanotube membranes are mechanically robust and can be obtained over a large area. It was found that the size of the opened tube mouth can be readily adjusted by the applied voltage pulses, thus making the resulting nanotube membranes favorable for use in bioseparation. More importantly, the in situ separation process allows continuous fabrication of such free-standing, through-hole TiO_2 nanotube array membranes. In addition, these nanotube membranes can be used to prepare interdigitated heterojunction nanocables and are expected to find potential applications in various photoelectric devices, flow-through photocatalysis, and bioinfiltration.

Introduction

Well aligned TiO_2 nanotube (NT) arrays fabricated by electrochemical anodization have attracted tremendous interest in recent years because of their remarkably enhanced photoelectric properties and technological importance for various applications, including solar cells, photocatalysis, gas sensors, water splitting, and functional surface devices.^{1–7} For example, in combination with p-type semiconducting materials, the vertically oriented TiO_2 NT arrays have been proved to be promising photoelectrodes for solid-state solar cells in which photon-induced excitons can be effectively separated and quickly transported.^{8,9} However, developing TiO_2 NT based composites still remains challenging so far because of the difficulty in filling the as-prepared TiO_2 nanotubes by usual spin-coating and electrochemical deposition methods.

In general, the TiO_2 NTs fabricated by anodization are attached to the underlying Ti substrate, and the bottom of

the tubes is closed with a barrier layer. In most cases, the use of this material is based on the configuration of TiO_2 NT array supported on Ti substrate (TiO_2 NTs/Ti). For solar cell application, however, the opaque Ti substrate precludes the use of front illumination geometry (light is incident through the TiO_2 electrode), and only allows illumination coming through the counter electrode (back illumination), which severely limits the cell's efficiency because of light losses.¹⁰ Electrochemical growth of TiO_2 NT arrays on a transparent conductive oxide substrate (e.g., FTO or ITO) may overcome this problem, but the length of the NTs is substantially limited by the obstacle in growing a high quality, thick Ti film on the conductive glass.¹¹ To get a better solution, a free-standing (self-supporting) and transparent TiO_2 NT array membrane with tunable tube lengths (i.e., membrane thickness) is strongly needed. In addition to the use in solar cells, free-standing TiO_2 NT membranes with through-hole morphology would also be favorable for many other applications such as nanoreactors, bioinfiltration, and flow-through photocatalytic reactions.^{12,13} So far, there are only few attempts dedicated to the fabrication of free-standing, through-hole TiO_2 NT array membranes,^{14–16} which primarily involve the selective dissolution of the supporting Ti substrate, followed by the removal of the

*To whom correspondence should be addressed. E-mail: liulif@mpi-halle.de.

(1) Mor, G. K.; Shankar, K.; Paulose, M.; Varghese, O. K.; Grimes, C. A. *Nano Lett.* **2006**, *6*, 215.

(2) Kuang, D.; Brillet, J.; Chen, P.; Takata, M.; Uchida, S.; Miura, H.; Sumioka, K.; Zakeeruddin, S. M.; Grätzel, M. *ACS Nano* **2008**, *2*, 1113.

(3) Albu, S. P.; Ghicov, A.; Macak, J. M.; Hahn, R.; Schmuki, P. *Nano Lett.* **2007**, *7*, 1286.

(4) Paulose, M.; Varghese, O. K.; Mor, G. K.; Grimes, C. A.; Ong, K. G. *Nanotechnology* **2006**, *17*, 398.

(5) Mor, G. K.; Shankar, K.; Paulose, M.; Varghese, O. K.; Grimes, C. A. *Nano Lett.* **2005**, *5*, 191.

(6) Zheng, Q.; Zhou, B.; Bai, J.; Li, L.; Jin, Z.; Zhang, Z.; Li, J.; Liu, Y.; Cai, W.; Zhu, X. *Adv. Mater.* **2008**, *20*, 1044.

(7) Wang, D.; Liu, Y.; Liu, X.; Zhou, F.; Liu, W.; Xue, Q. *Chem. Commun.* **2009**, 7018.

(8) Mor, G. K.; Kim, S.; Paulose, M.; Varghese, O. K.; Shankar, K.; Basham, J.; Grimes, C. A. *Nano Lett.* **2009**, *9*, 4250.

(9) Wang, Q.; Zhu, K.; Neale, N. R.; Frank, A. J. *Nano Lett.* **2009**, *9*, 806.

(10) Rani, S.; Roy, S. C.; Paulose, M.; Varghese, O. K.; Mor, G. K.; Kim, S.; Yoriya, S.; LaTempa, T. J.; Grimes, C. A. *Phys. Chem. Chem. Phys.* **2010**, *12*, 2780.

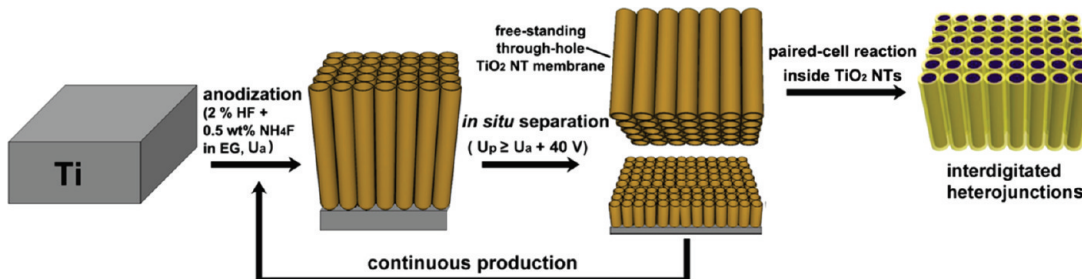
(11) Varghese, O. K.; Paulose, M.; Grimes, C. A. *Nat. Nanotechnol.* **2009**, *4*, 592.

(12) Paulose, M.; Peng, L.; Popat, K. C.; Varghese, O. K.; LaTempa, T. J.; Bao, N.; Desai, T. A.; Grimes, C. A. *J. Membr. Sci.* **2008**, *319*, 199.

(13) Varghese, O. K.; Paulose, M.; LaTempa, T. A.; Grimes, C. A. *Nano Lett.* **2009**, *9*, 731.

(14) Paulose, M.; Prakasam, H. E.; Varghese, O. K.; Peng, L.; Popat, K. C.; Mor, G. K.; Desai, T. A.; Grimes, C. A. *J. Phys. Chem. C* **2007**, *111*, 14992.

Scheme 1. Schematic Illustration of the Fabrication Process of the Free-Standing and through-Hole TiO_2 Nanotube Array Membranes and Interdigitated Heterojunctions



barrier layer by chemical etching. This process is tedious and involves the use of environmentally unfriendly hydrogen fluoride. Moreover, it was often observed that the bottom morphology of the NTs turned to be inhomogeneous after pore-opening.¹⁵ Recently, Losic et al. reported the preparation of the through-hole TiO_2 NT membranes by stepwise voltage reduction,¹⁶ a well-established method for obtaining free-standing and through-hole porous alumina membranes. However, after intensive investigations we found that this technique does not work well for Ti anodization, probably because of the different anodizing styles between Al and Ti. Moreover, it was also very hard to obtain large-area TiO_2 NT array membranes with high quality because of the required ultrasonication treatment. Other attempts including complete anodization of a Ti foil, were also made,¹⁷ nevertheless, the fabrication of free-standing, through-hole TiO_2 NT array membranes over a large area, still remains a challenge.

On the other hand, as a multifunctional n-type semiconductor material, anodized free-standing TiO_2 NTs are also very useful in various application designs such as photocatalysts, electrochemical sensors, and deposition templates.^{18,19} However, there are only a few reports about the applications of this free-standing film because of the fragile nature of TiO_2 membrane. Furthermore, there is still no a reliable technology to produce free-standing TiO_2 NT array membrane with a large area, structural integrity, and also low cost, similar as the commercial anodic aluminum oxide templates. Here, we report a novel strategy for the continuous fabrication of free-standing TiO_2 NT array membranes with controllable through-hole morphology over a large area. As an application example, we used them as templates and n-type nanomaterial to form the interdigitated heterojunctions by a simple paired-cell reaction through ion migration. It is expected that the large contact interface and ordered structure of these coaxial heterojunctions may greatly facilitate the creation of photon-induced excitons and accelerate the electro-hole separation and transport in the photoelectronic devices.

Experimental Section

Free-Standing and Through-Hole TiO_2 NT Membrane. Highly ordered TiO_2 NTs were prepared by potentiostatic anodization in a two-electrode electrochemical cell. All the anodization experiments were carried out at room temperature using commercially available Ti foil (Sigma-Aldrich, purity 99.7%) as a working electrode, and a Pt plate as a counter electrode. Before use, the Ti substrates were washed with ethanol, acetone, and distilled water in sequence, and then subjected to ultrasonication treatment for several minutes. To effectively reduce defects on the surface, the Ti foils were preanodized in a 0.5 wt % NH_4F ethylene glycol solution at 60 V for 4 h. The resulting TiO_2 NT layer was then removed by ultrasonication in 1 M HCl aqueous solution. Subsequently, the textured Ti substrates were anodized for the second time in the ethylene glycol electrolyte containing 2 vol % HF (37%), and 0.5 wt % NH_4F at $U_a = 60\text{--}90$ V for 1 h. At the end of the anodization, a larger anodic voltage ($U_p \geq U_a + 40$ V) was applied for a short time to get the free-standing and through-hole TiO_2 NT array membranes.

Formation of Interdigitated Heterojunctions. The $\text{Cu}_{2-x}\text{S}@\text{TiO}_2$ nanojunctions were prepared via the chemical reaction between Cu^{2+} and S^{2-} inside the through-hole TiO_2 nanotubes which were sandwiched between two half cells, one containing 0.01 M CuCl_2 and the other 0.01 M Na_2S . The growth of Cu_{2-x}S nanowire cores/nanoshell took place at room temperature, and the duration was around 12 h using a free-standing and through-hole TiO_2 NT membrane with or without the top porous layer as templates.

Characterization. The morphologies of the as-prepared TiO_2 NTs and $\text{Cu}_{2-x}\text{S}@\text{TiO}_2$ nanohybrids were examined by scanning electron microscopy (SEM, JEOL-6701F). The microstructures and composition of the $\text{Cu}_{2-x}\text{S}@\text{TiO}_2$ nanocables were further analyzed by transmission electron microscope (TEM, Philips CM20FEG) equipped with energy dispersive X-ray spectrometer (EDX). The nanocables were dispersed on a carbon-coated Mo TEM grid for the investigation.

Results and Discussion

As illustrated in Scheme 1, the fabrication is accomplished by a conventional anodization of Ti in ethylene glycol containing 2 vol % HF and 0.5 wt % NH_4F at a constant voltage U_a ,²⁰ immediately followed by the application of a large anodic voltage pulse (U_p , $U_p \geq U_a + 40$ V) for a short time. This results in the in situ separation of an intact TiO_2 NT array membrane over the whole anodized area, leaving behind a thin fresh NT layer

(15) Albu, S. P.; Ghicov, A.; Macak, J. M.; Hahn, R.; Schmuki, P. *Nano Lett.* **2007**, *7*, 1286.
 (16) Kant, K.; Losic, D. *Phys. Status Solidi RRL* **2009**, *3*, 139.
 (17) Kim, D.; Lee, K.; Roy, P.; Birajdar, B. I.; Specker, E.; Schmuki, P. *Angew. Chem., Int. Ed.* **2009**, *48*, 9326.
 (18) Ghicov, A.; Schmuki, P. *Chem. Commun.* **2009**, 2791.
 (19) Seabold, J. A.; Shankar, K.; Wilke, R. H. T.; Paulose, M.; Varghese, O. K.; Grimes, C. A.; Choi, K.-S. *Chem. Mater.* **2008**, *20*, 5266.

(20) Wang, D.; Liu, Y.; Yu, B.; Zhou, F.; Liu, W. *Chem. Mater.* **2009**, *21*, 1198.

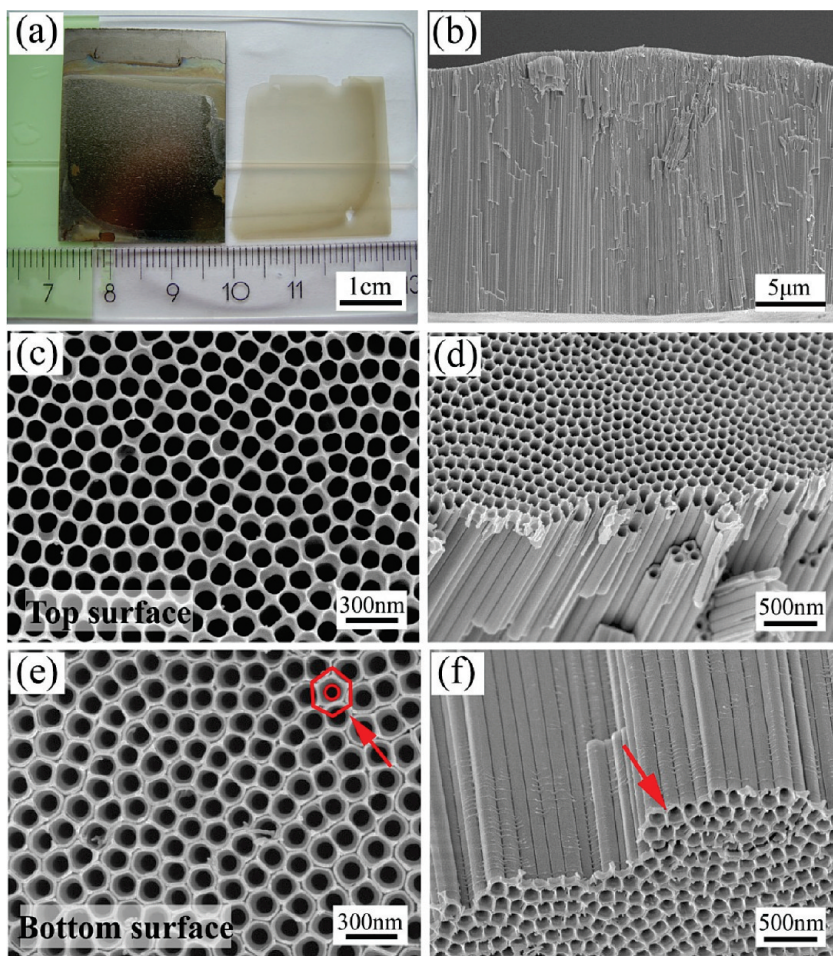


Figure 1. (a) Digital photograph of the separated free-standing TiO₂ nanotube array membrane. Left: Ti substrate. (b) Cross-sectional SEM image of the membrane. Plan-view and tilt-view SEM micrographs of (c, d) the top surface and (e, f) the bottom surface. The arrows indicate thin annulus standing on the tube wall.

remaining on the Ti substrate. Furthermore, the bottom of all NTs in the free-standing membrane turns out to be open upon separation, that is, the membrane is through-hole. The size of the opened tube bottom can be readily tuned by the applied voltage pulse U_p . In addition, the remaining Ti substrate can be directly used for the next run of anodization, thus allowing continuous production of free-standing TiO₂ NT array membranes with highly sequential quality. This *in situ* separation process is simple and remarkably reproducible, and also eliminates the need for environmentally unfriendly corrosive etching solutions.

Figure 1a shows a digital photograph of the as-prepared free-standing TiO₂ NT array membrane ($U_a = 80$ V for 1 h, $U_p = 180$ V for 20 s), the size of which is as large as 2.5 cm × 3 cm. It is clearly seen that the membrane is transparent and free of cracks. Moreover, it was observed that the free-standing membrane is mechanically robust and only slightly bending upon air drying, in stark contrast to the curling and fracture nature of the free-standing TiO₂ NT membranes reported before.¹⁷ This could be ascribed to the absence of barrier layer at the tube bottom in our samples so that there is smaller compressive stress exerted on the membranes. It is expected that by using the critical point drying method described by Paulose et al.,¹⁴ the membranes could remain fairly flat after drying. The

microscopic morphology of the TiO₂ NT array membrane was thoroughly examined by scanning electron microscopy, as depicted in Figure 1b–f. It is evident that the membrane consists of a dense array of well-aligned, through-hole TiO₂ NTs with a length of 18 μm (Figure 1b). All NTs were found to be open at both the top (Figure 1c–d) and bottom side (Figure 1e–f). Upon closer examination of the SEM micrographs, it is found that the morphology of the top surface is slightly different from that of the bottom. On the top surface, there exists a nanoporous layer (~200 nm thick),²⁰ which is analogous to the surface of porous anodic alumina.²¹ It is assumed that this nanoporous layer plays a critical role in maintaining the intactness of the free-standing membrane. In contrast, discrete and cylindrical tube-like features are clearly seen on the bottom surface. There are small gaps between the nanotubes on the new opened bottom surface. These gaps extend continuously between the top and bottom surfaces, especially for the TiO₂ NTs without top porous layer (shown in Supporting Information, Figure S1). This would be favorable for the deposition of sandwich-like heterojunctions by ion migration

(21) Liu, L.; Lee, S. W.; Li, J. B.; Alexe, M.; Rao, G. H.; Zhou, W. Y.; Lee, J. J.; Lee, W.; Gösele, U. *Nanotechnology* **2008**, *19*, 495706.

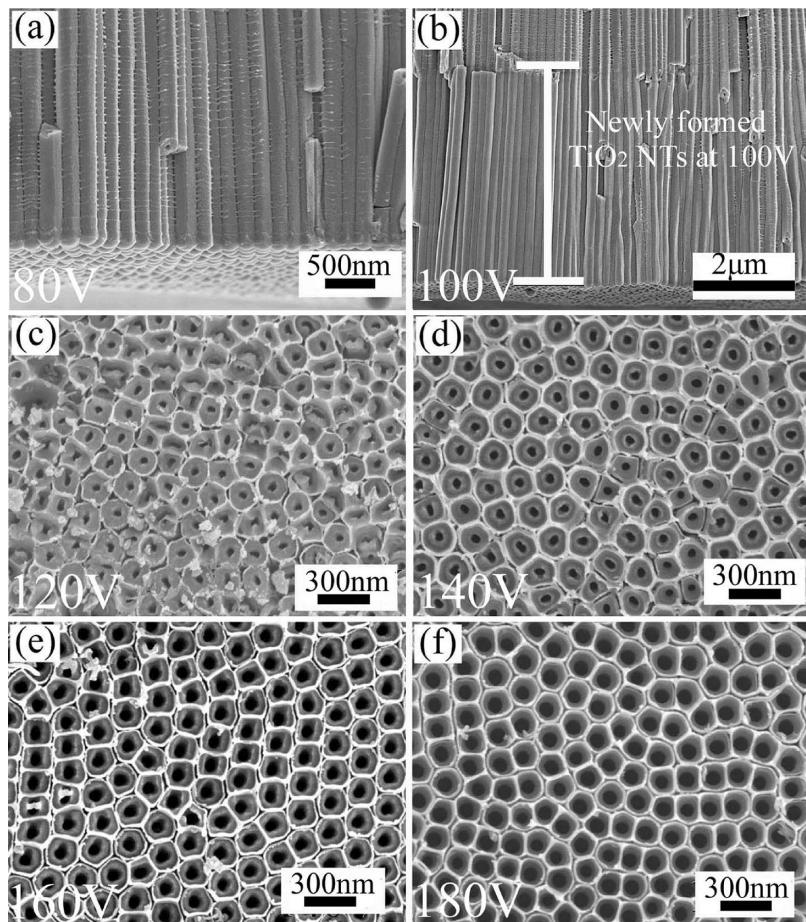


Figure 2. Effects of the applied anodic voltage pulses on the diameter of the tube mouth at the bottom of the through-hole TiO_2 NT membrane.

deposition. Moreover, it was observed that there is a thin annulus standing on the tube wall of each NT at the bottom, which could result from the high voltage pulse induced *in situ* separation process (Figure 1e–f, details will be discussed below). Extensive SEM examinations confirmed that the bottom of the NTs are uniformly opened over the whole TiO_2 NT membrane (Supporting Information, Figure S2), and no morphological inhomogeneity, like that reported previously,¹⁵ was observed.

To get free-standing and through-hole TiO_2 NT array membranes, the applied pulse voltage has to be carefully chosen. It was found that only with the difference between U_a (conventional anodization voltage, 50–90 V) and U_p (anodic voltage pulse) being larger than 40 V, a large area free-standing NT membrane can be obtained. A voltage pulse of $U_p < U_a + 40$ V only results in continuous growth of TiO_2 NTs, instead of the separation of a free-standing membrane. Figure 2 illustrates the effect of different anodic voltage pulses U_p on the bottom morphology of the membranes. The membranes were prepared by a conventional anodization at $U_a = 80$ V for 1 h, followed by the application of U_p at 80 V, 100 V, 120 V, 140 V, 160 V, and 180 V, respectively, for 5 min (Figure 2a–b) or until the membranes were separated from the Ti substrate (Figure 2c–f). It is evident from Figure 2a that $U_p = 80$ V gives rise to neither discernible morphological change nor the opened tube bottom. When $U_p = 100$ V was applied,

continuous growth of TiO_2 NTs, rather than membrane separation, was clearly observed, which can be distinguished by a visible interface between the NT layer formed at $U_a = 80$ V and the NT layer formed at $U_p = 100$ V, as is shown in Figure 2b. In contrast, when $U_p \geq 120$ V (i.e., $U_p \geq U_a + 40$ V), the separation of free-standing TiO_2 NT membranes with through-hole morphology from the Ti substrates were exclusively observed (Figure 2c–f). Furthermore, it was found that the average diameter of the tube mouth increases with the increasing pulse voltages, being 40 nm for $U_p = 120$ V, 49 nm for $U_p = 140$ V, 77 nm for $U_p = 160$ V, and 88 nm for $U_p = 180$ V, respectively. The monotonic increase of the tube mouth size with U_p might be associated with the enhancement of electric field assisted etching under a high anodic voltage. In addition, the separation rate was also found to be closely related to U_p . For $U_p = 180$ V, a free-standing NT array membrane can be detached from the Ti substrate within 20 s; while for $U_p = 120$ V, complete separation of a free-standing membrane typically takes 2–3 min. So, the diameter of the opened mouth can be well controlled by adjusting the applied voltage. The free-standing TiO_2 NT membranes with controllable tube mouth size at their bottom will be particularly useful for the bioinfiltration application.

Since the geometrical parameters (except the tube mouth size at the bottom side) of the TiO_2 NT arrays

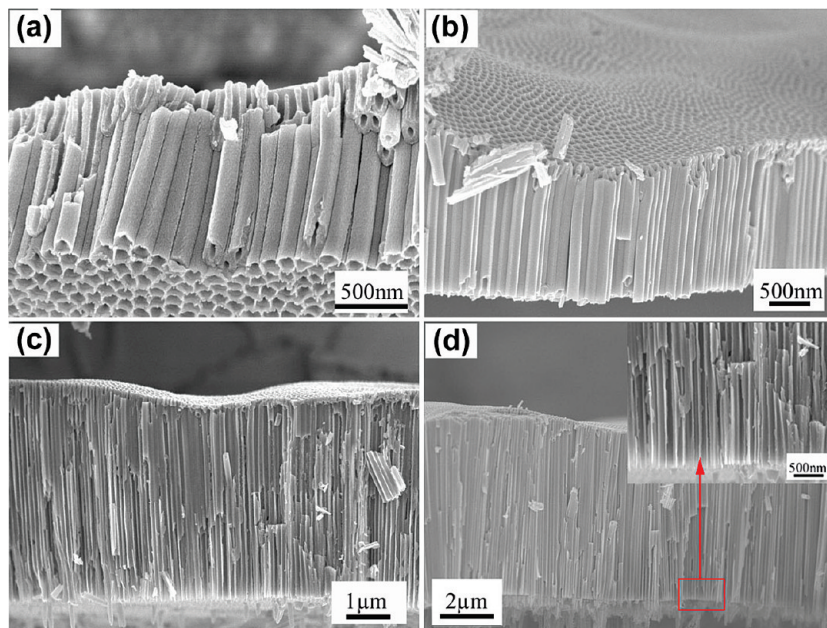
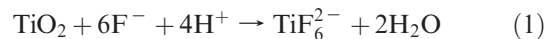


Figure 3. Thin free-standing and through-hole TiO₂ NT array membranes prepared with $U_a = 80$ V for (a) 1 min (1 μ m), (b) 2 min (1.8 μ m), (c) 5 min (4 μ m), and (d) 10 min (7 μ m), followed by the application of $U_p = 180$ V for 20 s.

are mainly governed by conventional anodization conditions (e.g., U_a) and independent of U_p , free-standing, through-hole TiO₂ NT array membranes with tunable tube diameter, tube wall thickness, and tube length (i.e., membrane thickness) can be readily obtained by changing the conventional anodization conditions such as U_a , temperature, electrolyte concentrations, and pH.^{20,22–24} In particular, free-standing, through-hole TiO₂ NT array membranes as thin as several micrometers, which are quite difficult to obtain by conventional separation methods because of the fragile nature and similar solubility of TiO₂ and the Ti substrate, can also be easily achieved by the in situ separation process reported here (Figure 3). These thin membranes are mechanically robust and can be transferred onto any desired substrates, which may be potentially used as shadow masks to grow nanodot arrays.^{25,26}

To clarify the separation mechanism of the free-standing and through-hole NT membranes, we carried out a time-dependent investigation on the morphology evolution of the bottom of the NTs. To this end, an U_p of 140 V was applied immediately after the conventional anodization ($U_a = 80$ V) for 2 s, 5 s, 15 s, 30 s, and 50 s, respectively. The bottom morphologies of the resulting NTs were carefully examined by SEM. Figure 4 displays representative SEM images and the schemes showing the presumed separation mechanism. More SEM micrographs showing the morphological evolution of the NTs are presented in

Supporting Information, Figures S3 and S4. It is known that under a given temperature and electrolyte concentration, the anodization voltage usually governs the nucleation and growth of the TiO₂ NTs and determines the geometrical parameters such as tube diameter and intertube distance.²⁷ It is assumed that the abrupt change of electric field at the barrier layer as a result of the introduction of a large U_p breaks the originally established dynamic equilibrium between the Ti oxidation and dissolution of TiO₂, initiating the renucleation of TiO₂ NTs. However, unlike the nucleation process on a flat Ti surface, the renucleation upon the application of U_p is confined inside the formed NTs. To adapt to U_p , the newly established electric field tends to intensify laterally, and thus splits each barrier layer into several smaller pits, as evidenced from Figure 4b. Correspondingly, the individual barrier layer turns to be spherical and well separated from each other. However, because of the interaction among the neighboring NTs, the renucleation process would not proceed laterally. Instead, the electric field will drive these small pits to develop vertically into small-diameter NTs (Figure 4c–e). In the meantime, the part connecting the original NTs and the newly formed small NTs is undermined with the enhanced field-assisted dissolution resulting from the drastic increase of F[−] concentration at the tube bottom upon the application of U_p , as described by reaction 1,²⁸ finally leading to the detachment of the originally formed NT array and leaving behind a thin small-diameter NT layer on the Ti substrate (Figure 5).



- (22) Wang, D.; Yu, B.; Wang, C.; Zhou, F.; Liu, W. *Adv. Mater.* **2009**, *21*, 1964.
- (23) Paulose, M.; Shankar, K.; Yoriya, S.; Prakasam, H. E.; Varghese, O. K.; Mor, G. K.; Latempa, T. A.; Fitzgerald, A.; Grimes, C. A. *J. Phys. Chem. B* **2006**, *110*, 16179.
- (24) Kaneko, S.; Chen, Y.; Westerhof, P.; Crittenden, J. C. *Scr. Mater.* **2007**, *56*, 373.
- (25) Rodriguez, B. J.; Gao, X. S.; Liu, L. F.; Lee, W.; Naumov, I. I.; Bratkovsky, A. M.; Hesse, D.; Alexe, M. *Nano Lett.* **2009**, *9*, 1127.
- (26) Gao, X. S.; Liu, L. F.; Birajdar, B.; Ziese, M.; Lee, W.; Alexe, M.; Hesse, D. *Adv. Funct. Mater.* **2009**, *19*, 3450.

- (27) Mor, G. K.; Varghese, O. K.; Paulose, M.; Shankar, K.; Grimes, C. A. *Sol. Energy Mater. Sol. Cells* **2006**, *90*, 2011.

- (28) Macak, J. M.; Tsuchiya, H.; Ghicov, A.; Yasuda, K.; Hahn, R.; Bauer, S.; Schmuki, P. *Curr. Opin. Solid State Mater. Sci.* **2007**, *11*, 3.

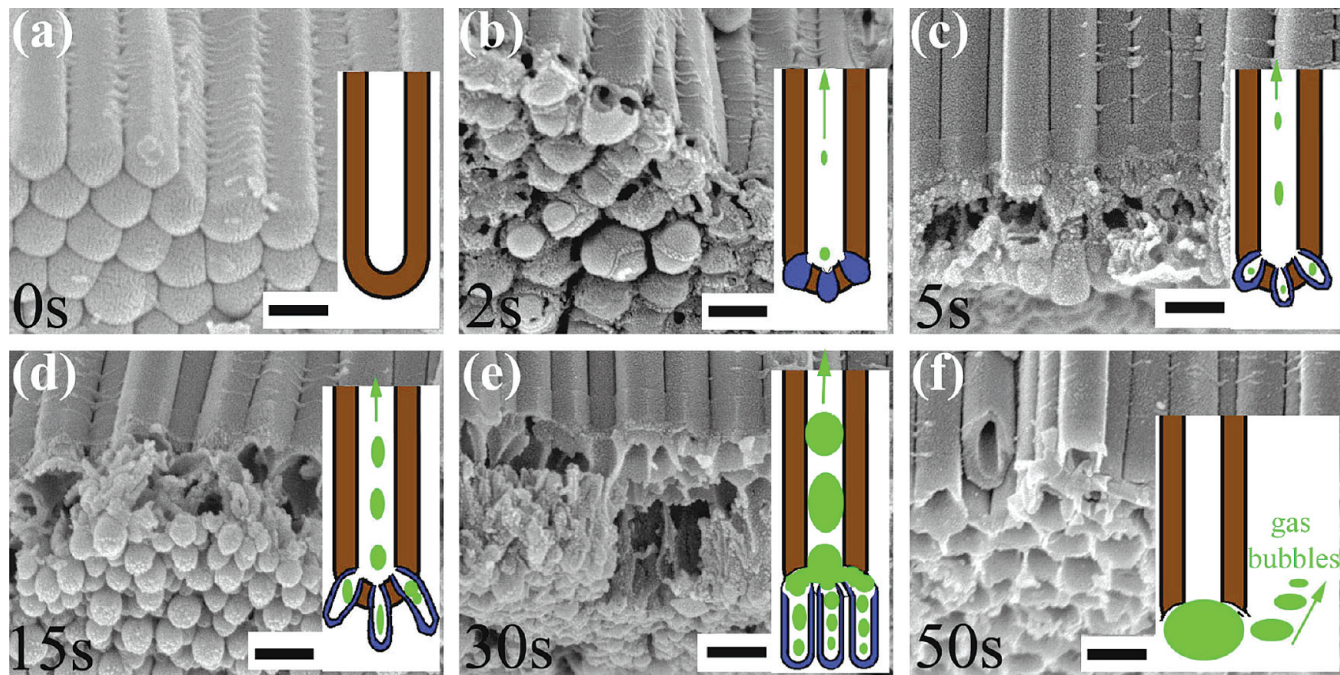


Figure 4. Time-dependent bottom morphologies of the TiO_2 NTs upon the application of a voltage pulse of 140 V for (a) 0 s, (b) 2 s, (c) 5 s, (d) 15 s, (e) 30 s, and (f) 50 s. The insets show the schemes of the presumed separation mechanism of the free-standing, through-hole TiO_2 NT membrane. The scale bars correspond to 200 nm.

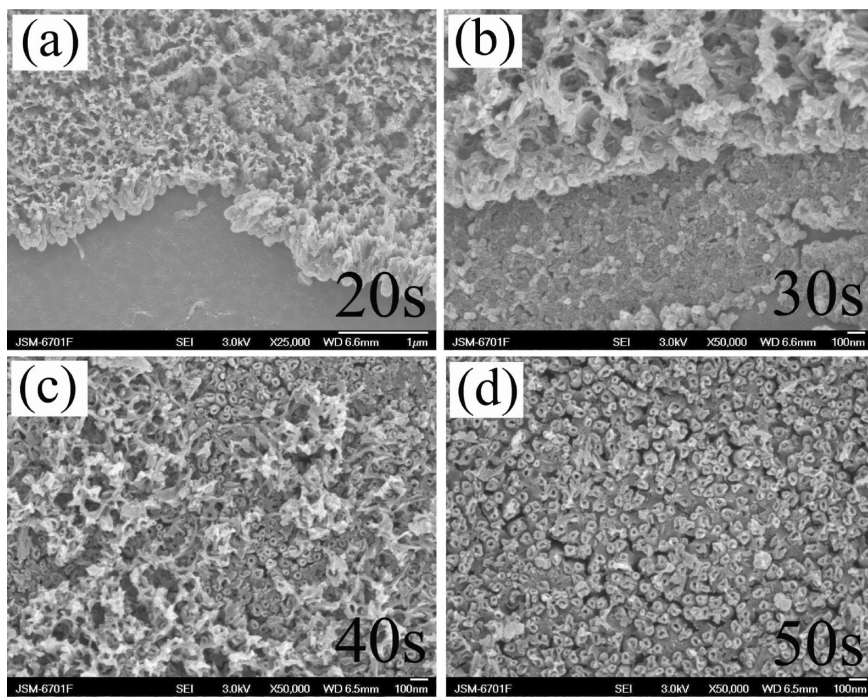


Figure 5. Top-view SEM images of the surface of the Ti substrates after the separation of TiO_2 NT membranes. The separation of free-standing membranes was realized by the application of a voltage pulse of 140 V for (a) 20 s; (b) 30 s; (c) 40 s, and (d) 50 s.

Aside from the enhanced field-assisted dissolution, it is believed that the stresses due to the significantly enhanced volume expansion upon the application of U_p also play an important role in the detachment process. It is known that the compressive stress during anodizing increases with current density. Once U_p was applied, the abruptly increased current density would introduce a large compressive stress at the metal-film interface which could induce separation. In addition, the overall process was found to be accompanied

with the evolution of gas bubbles (which presumably are O_2 from the oxidation of oxygenated species at the anode),^{29,30} which can also help the separation of through-hole TiO_2 NT film from the substrate (see the schemes in Figure 4). Phenomenologically, it was observed that at first a large

(29) Lee, W.; Scholz, R.; Gösele, U. *Nano Lett.* **2008**, *8*, 2155.

(30) Crossland, A. C.; Habazaki, H.; Shimizu, K.; Skeldon, P.; Thompson, G. E.; Wood, G. C.; Zhou, X.; Smith, C. J. E. *Corros. Sci.* **1999**, *41*, 1945.

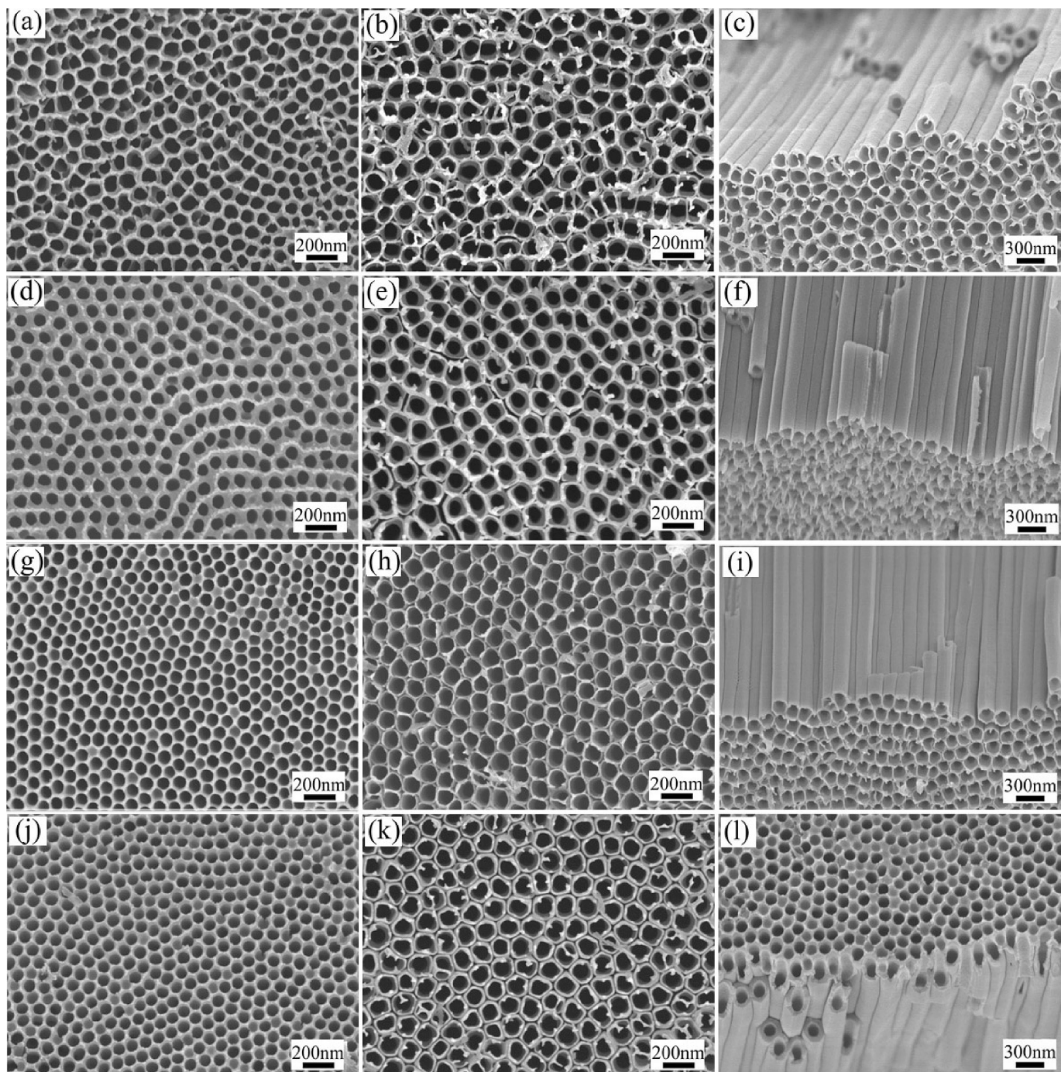


Figure 6. Continuous production of free-standing, through-hole TiO_2 NT array membranes with the same Ti substrate for four cycles (1th: a–c; 2nd: d–f; 3rd: g–i; 4th: j–l). SEM micrographs of the membranes (a, d, g, j) Top surface. (b, e, h, k) bottom surface. (c, f, i, l) side-view.

density of small gas bubbles emerged once U_p was applied. They then quickly coalesced into bigger ones and gradually spread over the whole anodized area, and eventually pushing the NT membrane away from the Ti substrate.

It is worth mentioning that the in situ separation process allows continuous production of free-standing, through-hole TiO_2 NT array membranes with designed geometries in an economical manner, rendering maximum utilization of the Ti substrate, and therefore holds great promise for widespread commercialization. Figure 6 shows representative SEM micrographs of the free-standing TiO_2 NT array membranes prepared with the same Ti substrate for four cycles in sequence. The membranes were obtained by a conventional anodization at $U_a = 70$ V for 1 h, followed by an in situ separation with $U_p = 220$ V. It is clear that the morphology of these four membranes looks quite similar. All membranes consist of a dense array of NTs with well-defined open-ended morphology at their tops and bottoms. It is also noted that the membranes fabricated in latter cycles exhibit much improved spatial ordering in terms of the arrangement of the NTs, which could be associated with the reduced defect density on the textured Ti surface.

As mentioned above, the free-standing, through-hole TiO_2 NT membranes can be used as templates for the fabrication heterojunction nanocables. TiO_2 NT based heterostructures have recently attracted increasing interest for use in all-solid-state heterojunction solar cells because they are good one-dimensional electron conductors, very stable, and resistant to environment attacks. On the other hand, more and more semiconducting metal sulfide nanomaterials (e.g., CdS , CuS , Cu_2S , PbS) possessing novel optical and electrical properties are considered as promising active components in various photovoltaic devices such as dye-sensitized solar cells, inorganic–inorganic solar cells, and hybrid nanocrystal-polymer composite solar cells. However, the formation of well-defined TiO_2 NTs/metal sulfides still remains a challenging task albeit some functional hybrid nanostructures such as interdigitated $\text{CdS}@\text{TiO}_2$, $\text{CdTe}@\text{TiO}_2$, $\text{CuInSe}_2@\text{TiO}_2$, or $\text{P}3\text{HT}@\text{TiO}_2$ heterostructure arrays have been achieved.^{19,31,32} Recently, template directed paired-cell

(31) Wang, D.; Liu, Y.; Wang, C.; Zhou, F.; Liu, W. *ACS Nano* **2009**, *3*, 1249.

(32) Zhu, W.; Liu, X.; Liu, H.; Tong, D.; Yang, J.; Peng, J. *J. Am. Chem. Soc.* **2010**, *132*, 12619.

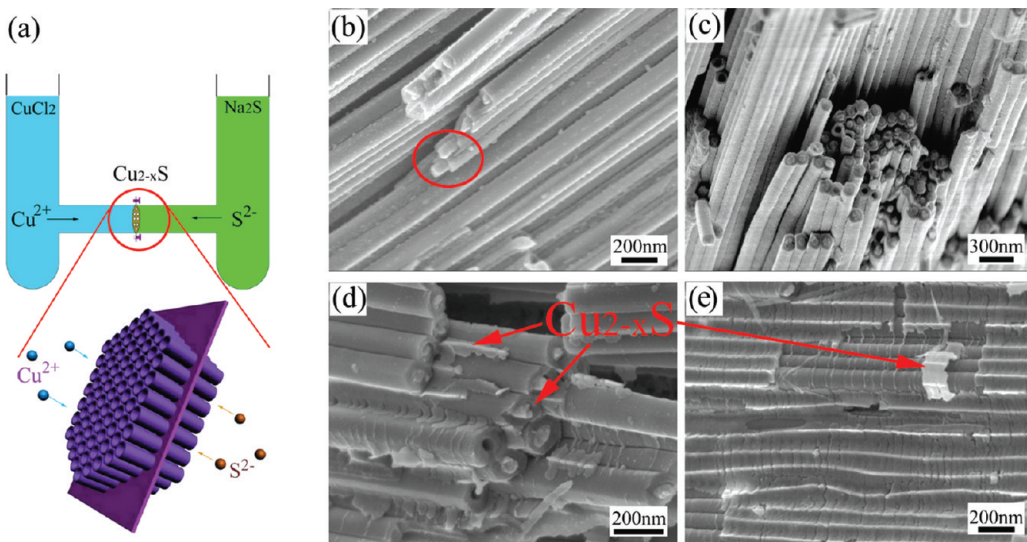


Figure 7. Fabrication of the interdigitated Cu_{2-x}S@TiO₂ nanohybrids. (a) Schematic illustration of the fabrication. SEM images of (b, c) the Cu_{2-x}S@TiO₂ nanocables, and (d, e) Cu_{2-x}S@TiO₂@Cu_{2-x}S trilayer nanocables.

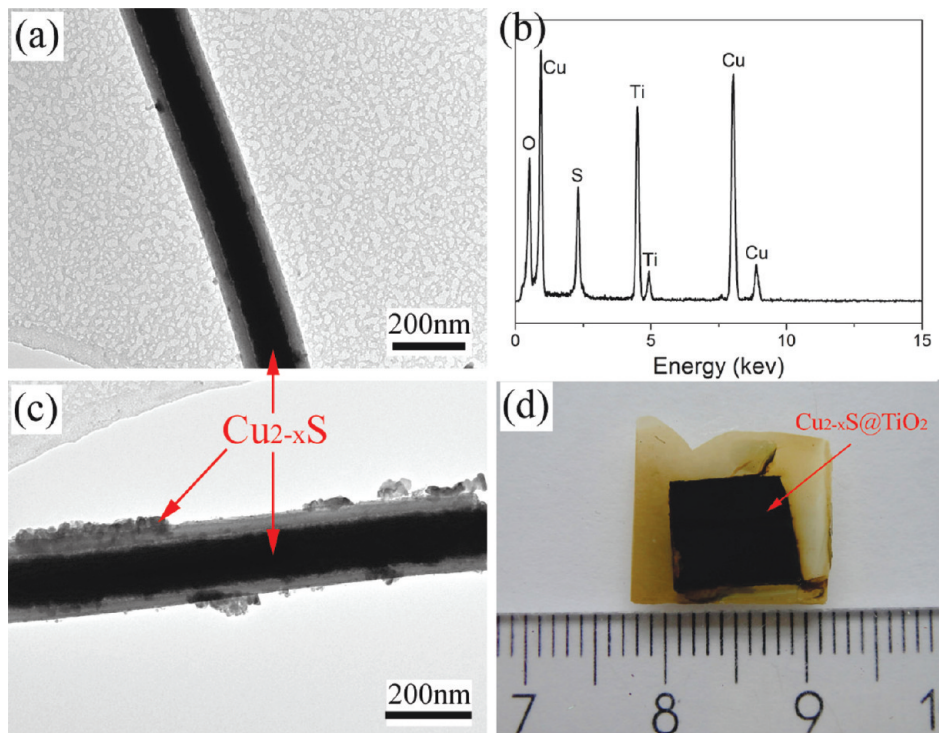


Figure 8. (a) TEM image of Cu_{2-x}S@TiO₂ nanocable; (b) EDX spectrum shown in (a); (c) TEM image of Cu_{2-x}S@TiO₂@Cu_{2-x}S composite material; (d) a photograph of the as prepared Cu_{2-x}S@TiO₂ nanomaterial prepared by paired-cell reaction using the through-hole TiO₂ NTs as nanoreactors.

reaction using through-hole porous anodic aluminum oxide or polycarbonate membranes as nanoreactors has been proved to be a straightforward and effective route for the fabrication of nano-objects.^{33–36} Inspired by this, we demonstrate here for the first time that with the as-prepared free-standing, through-hole TiO₂ NT membrane serving as a template and an array of nanoscale reactors, the interdigitated Cu_{2-x}S@TiO₂ radial composite nanocables can be easily realized by the chemical reac-

tion between Cu²⁺ and S²⁻ inside the TiO₂ NTs which were sandwiched between the two half cells (Figure 7a), one containing CuCl₂ and the other Na₂S. Figures 7b and 7c show the representative SEM images of the as-prepared Cu_{2-x}S@TiO₂ nanocables with a high filling degree using a top porous free-standing TiO₂ NTs membrane as the template and the n-type semiconductor, from which the core–shell structure can be clearly distinguished. Interestingly, the sandwich-like trilayer Cu_{2-x}S nanowire@TiO₂ NT@Cu_{2-x}S shell heterojunction nanocables can also be formed by this method using through-hole TiO₂ NT membranes without top porous layer (Supporting Information, Figure S1) as the template. The result shows that apart

(33) Mao, Y.; Wong, S. S. *J. Am. Chem. Soc.* **2004**, *126*, 15245.

(34) Mao, Y.; Wong, S. S. *J. Am. Chem. Soc.* **2006**, *128*, 8217.

(35) Zhou, H.; Wong, S. S. *ACS Nano* **2008**, *2*, 944.

(36) Zhang, F.; Wong, S. S. *Chem. Mater.* **2009**, *21*, 4541.

from the reaction occurring inside the NTs, the Cu^{2+} and S^{2-} can also move into the small gaps among the TiO_2 NTs by ion migration to form a continuous shell structure. This sandwich-like structure can greatly enhance the contact area between the two materials, and thus is expected to exhibit improved photoelectric properties.

It is also worth mentioning that unlike other impregnation methods which either render an incomplete filling or lead to lose contact between the guest and host materials, the as-formed Cu_{2-x}S has a very close contact with the TiO_2 NTs over a long distance which can be seen from the TEM images in Figures 8a and 8c. The EDX analysis confirmed that the nanocables consist of O, S, Cu and Ti, as displayed in Figure 8c. Figure 8d shows a digital photograph of the as-prepared $\text{Cu}_{2-x}\text{S}@\text{TiO}_2$ nanocables. Detailed study of photoelectric properties of the interdigitated heterojunctions and exploration of other complex nanocables are under investigation. We believe that as a new structured template, the free-standing and through-hole TiO_2 NT membrane can be widely used to prepare other interdigitated heterojunctions by this simple and general method. Furthermore, multi-layered heterojunctions with two or more semiconductors could also be realized by sequential paired-cell reactions. It is expected that these interdigitated heterojunctions may find potential applications in solid-state heterojunction solar cells and photoelectric diodes.

Conclusions

In summary, we have developed a facile *in situ* separation procedure for the fabrication of large area free-standing TiO_2 NT array membranes with controllable through-hole morphology. Electric field induced branching of the barrier layer and the enhanced field-assisted dissolution, in conjunction with the evolution of excessive gas bubbles, are thought to be responsible for the *in situ* separation of the TiO_2 NT membranes. The process reported here is very simple and environmentally friendly, and more importantly allows the continuous production of free-standing and through-hole TiO_2 NT membranes. As a new and important semiconducting template material, these free-standing TiO_2 NT membranes can be used as effective nanoreactors to fabricate interdigitated nanocables and find potential applications in various photoelectric devices, flow-through photocatalysis and bioinfiltration.

Acknowledgment. The authors thank Dr. Mato Knez for his fruitful discussions.

Supporting Information Available: FESEM images of the free-standing and through-hole TiO_2 NTs with large area and controllable morphology, and EDS analysis of the $\text{Cu}_{2-x}\text{S}@\text{TiO}_2$ heterojunction, and so forth. This material is available free of charge via the Internet at <http://pubs.acs.org>.